2023 IEEE International Conference on Robotics and Automation (ICRA 2023)
May 29 - June 2, 2023. London, UK

Embedded active stiffening mechanisms to modulate Kresling tower kinetostatic properties

John Berre[1*], Lennart Rubbert[1], François Geiskopf[1] and Pierre Renaud[1]

***Abstract*— Non-rigidly foldable origamis are of great interest to build robotic components, as they are light, offer large deployability and can also be multistable. In this paper, we consider the Kresling tower, and propose an original way to actively modulate its kinetostatic properties. Actuated stiffening mechanisms are embedded on some folds of the origami. By adjusting the axial stiffness of the folds, modulation of the axial stiffness and the force required to switch between stable configurations are demonstrated. This adjustment can in addition be performed independently from the height of the stable configurations, which makes it simple to use. The interest of fold stiffening is outlined experimentally. Three actuation strategies are considered and implemented. Impact on Kresling tower properties are shown, with complementary performances of pneumatic, SMA-based and DC motor actuation.**

I. Introduction

Origami-inspired mechanisms are considered today in manipulation [1], mobile [2] or medical robotics [3], among others. Origami construction is based on the folding of a planar pattern to form a set of panels and folds in 3D. This process allows to produce lightweight mechanisms compared to their volume. Assembly in parallel of folds and panels allows them to be considered for tasks where stiffness [4] and load capacity in comparison with their weight [5], [6] are important, while offering large motions and shape changing capabilities.

The class of non-rigidly foldable origamis [7] is particularly interesting for robotics. For such origamis, the 3D configuration change implies deformations of the structure. This leads to structures that can be, in addition to the above-mentioned properties, bistable or even multistable [8]. For instance, the Kresling tower has been exploited in mobile [2], [9] and medical [3] robotics. Its behavior depends on the pattern geometry and also the stiffness of its folds and panels [10], [11]. This means the position of the stable configurations, the stiffness in these configurations, the force needed to switch between them, and more generally the kinetostatic model of non-rigidly foldable origamis can be modified by adjusting fold and panel stiffness [12].

Dynamically adjusting the kinetostatic model can be of great interest. A non-rigidly foldable origami could then be used for instance as a structural element with safety features such as stiffness variation, or integrated force limiter, for collaborative robots. This is our focus, for which different approaches could be applicable. In [13], [14], an external vacuum-activated structure is added around origamis. It allows a modulation of stiffness, but the external system might interfere with the origami free motion. In [15], the authors propose to lock the relative motion of panels by integrating SMA-based active elements along folds. The solution is compact, but mostly allows a binary operation. In [16], the torsional stiffness of origami folds is modulated. Stiffness variation is then possible. Such a torsional stiffness variation of the folds is also achieved in [17] using shape memory polymers. With the same technology, the ability to make a monostable or bistable origami is shown in [18], using a non-rigidly foldable origami. However, the position of stable configurations, the stiffness and forces to switch between stable configurations are coupled and cannot be set independently.

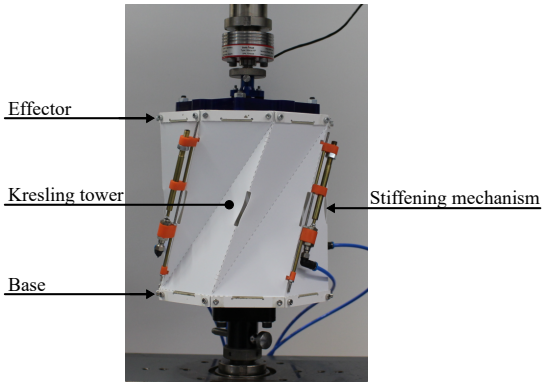

Fig. 1. Prototype of the proposed Kresling tower with embedded stiffening mechanisms during assessment.

In this paper, we propose to avoid these couplings and use an alternate approach to actively modify the kinetostatic model of non-rigidly foldable origamis. We focus on the Kresling tower, given its applicative interest. We have shown in [19] that the axial behavior of this origami can be significantly modified by making a simple local modification to the folds, via local openings. Stiffness and switching force, i.e. the force needed to get the transition between the two stable configurations, vary with the size of the opening, independently from the location of the stable configurations. Here, we propose to actively modify the impact of the openings, and by this way the tower behavior, by controlling the axial stiffness of the modified fold, instead of tuning the torsional stiffness. The targeted applications concern collaborative robotics, with stiffness control of structural elements as in [20], or bistability control of gripper as in [21]. The work is conducted with these applications in mind.

*Corresponding author: john.berre@insa-strasbourg.fr
[1]ICube - University of Strasbourg - CNRS - INSA Strasbourg
This work was supported by ANR (ORIGABOT ANR-18-CE33-0008), and the Investissements d'Avenir program (TIRREX ANR-21-ESRE-0015, Labex CAMI ANR-11-LABX-0004).

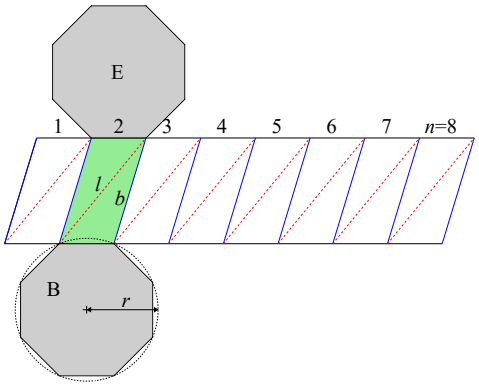

Fig. 2. The Kresling tower pattern with its parameterization.

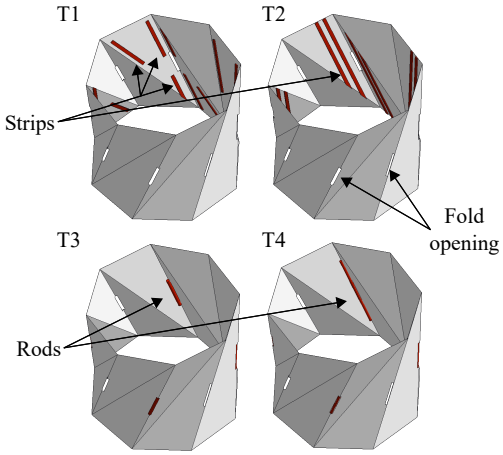

Fig. 3. Schematic representation of the 4 tested reinforcement modes: the stiffening components are in red. The attachments are not represented for sake of visibility.

The design process we adopted is mostly based on experimentation. The interest of integrating a solution on folds of the tower is put forward in section 2 through preliminary experiments. Then, the design of three active solutions is described in section 3, using pneumatic, electric and shape memory alloy actuation. An experimental characterization campaign is then set up in section 4 to discuss the contribution of the solutions and their respective interests given their different activation times, stiffness and bulk. Conclusions and perspectives are finally proposed in section 5.

II. Preliminary Evaluation for the Choice of the Stiffening Mode

A. Kresling tower and stiffening modes

The pattern of the Kresling tower is defined by a set of 4 parameters (l, b, r, n) shown in Fig. 2. Its lower and upper faces are considered respectively as the base B and the effector E. The effector has an helical motion [9]. The tower can exhibit bistable behavior with two equilibrium states, characterized by the height of the tower. Typical relationship between the force exerted on the effector and the height that characterizes the tower configuration is depicted in Fig. 4. The stable configurations correspond to two heights h_1 and

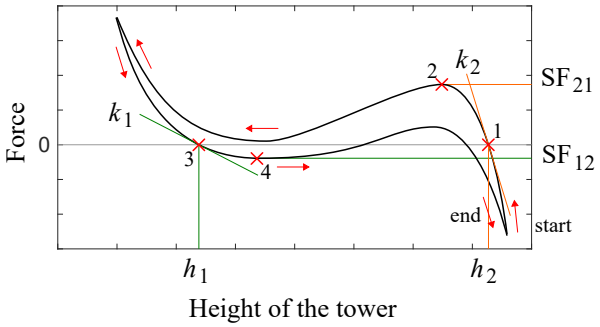

Fig. 4. Simplified representation of Kresling tower force-height relationship. The red arrows show the direction of travel. Points 1 to 4 are used to characterize the tower.

h_2. There is usually some dissipation in the system, so the loading and unloading phases are not superimposed. The mechanism bistability comes from the deformation under compression of the panels, which do not remain flat, and the folds, which do not remain straight. We have introduced in [19] a local fold opening, around the middle of the folds. It facilitates the deformation during the compression of the tower. The fold opening does not modify the location of stable configurations [19]. However, we could show it is possible to modify by design the other values of interest on the force-height relationship, shown in Fig. 4: the switching force to go from high to low (resp. low to high) configurations, denoted SF_{21} (resp. SF_{12}), the tower stiffness in low (resp. high) configurations k_1 (resp. k_2).

Our objective is to actively adjust these quantities. The proposition is then to place a mechanism in parallel to the fold opening, to modify the kinetostatic behavior of the tower. The Kresling tower has a complex motion, with large reconfigurations of the panels during the folding (see video). We want to place stiffening mechanisms directly on panels or folds, and not between the base and effector. In this way, the Kresling tower motion is not modified if the stiffening mechanisms are not activated. To achieve this, one can consider stiffening the panels, or stiffening the folds, as both are involved. Therefore, a preliminary experimental evaluation has been performed to identify the most relevant stiffening mode, and the best way to couple a stiffening solution to the origami.

B. Experimental evaluation

The Kresling tower we consider in the remaining of the paper is defined by (l, b, r, n)=(202.2 mm, 174.6 mm, 90 mm, 8), so that by design h_1 = 106.3 mm and h_2 = 166.3 mm. The local opening is 20% of the mountain fold length. Metal stiffeners, much more rigid than the polymer material of the tower, are placed on panels or folds to assess their impact. Four reinforced towers Ti, i$\in (1, 4)$ (Fig. 3, Table I), are compared before and after insertion of reinforcement elements. For panel stiffening (towers T1, T2), strips are inserted on panels adjacent to 4 mountain folds, one out of two. For fold stiffening (towers T3, T4), a set of 4 rods is inserted along the mountain folds, one out of two. In both

TABLE I

NATURE AND IMPACT OF REINFORCEMENTS. TYPE DESCRIBES THE REINFORCEMENT STRATEGY: P (RESP. F) IS PANEL (FOLD) STIFFENING. POSITION DESCRIBES THE ATTACHMENT MODE: G (RESP. L) IS FOR GLOBAL (LOCAL) ATTACHMENT ALONG PANEL/FOLD.

Tower	Type	Position	SF $[N]$	k_1 $[N/mm]$	k_2 $[N/mm]$
T1	P	L	+5.9	-0.1	-3.4
T2	P	G	+17.7	+0.5	+9.0
T3	F	L	+9.8	+0.2	+4.1
T4	F	G	>+22.6	+2.2	+11.6

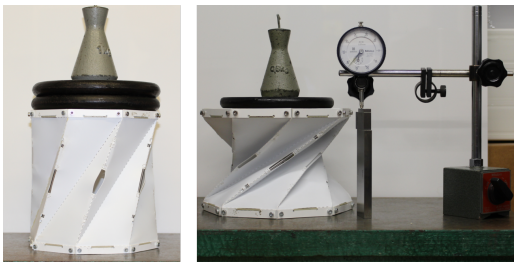

Fig. 5. Weight application to measure the switching force (left). Stiffness assessment for the low configuration (right).

cases, we consider either an attachment along the panel/fold length, or only locally around the fold opening. Towers are produced using polypropylene (PP), following [22]. The 0.5-mm thick PP sheet is laser cut (Speedy 300, Trotec Laser GmbH) with folds produced using a dashed profile [19].

The evaluation is conducted using two criteria: the switching force SF_{21} and the stiffness k_1 and k_2 in the two stable configurations. To assess the switching force, increasing weights are placed on the effector of the prototypes, until the switch is observed (Fig. 5). Weight increments are 100 g, and they are applied every 30 seconds to make experiments comparable, even in presence of material viscoelasticity. Experiments are stopped when reaching a weight of 6 kg, which is roughly twice the value for a tower without any stiffening, to avoid degradation of the prototypes. For height estimation, a dial indicator and gauge blocks are used. In a first step, the indicator probe is lightly applied on the tower effector using the adjustment wheel. This avoids to apply any significant force that would induce tower displacement. Then gauge blocks are used to determine the probe height. The process is repeated for 4 vertices of the origami, and the average height is reported. For stiffness estimation, a 1.5-kg weight is placed on top of the tower and measuring the resulting displacement of the effector as shown in Fig. 5. A 3-minute delay after weight application is respected, so all measurements are comparable.

The results are reported in Table I. The procedure was also used with reinforcement placed on 2 opposite and on all 8 mountain folds of the origami. Using 2 reinforcements has almost no effect. Using 8 reinforcements has an impact, but which is less than twice the variation introduced by 4 reinforcements. Only the results with 4 reinforcements are thus presented and discussed, because of the significant influence, without being a limitation in the study.

Attachment along the whole panel/fold has a greater impact than local attachment around the fold openings. The highest variations are observed with towers using reinforcements on the folds. In addition, we observed that anchoring the stiffeners on the panels is difficult to integrate because of space constraints. With T4 tower, the switching force is increased by more than 22.6 N with respect to the behavior of the tower without reinforcement. This represents a variation larger than 62%. Only the T4 tower allows to significantly increase the stiffness k_1. Similarly, the best results in terms of increase of k_2 stiffness are obtained with the T4 tower. The most interesting stiffening mode is thus to use stiffening mechanisms attached to the folds, along the maximum possible length.

III. DESIGN OF STIFFENING MECHANISMS

A. Operating principle

Given the initial observations, 4 identical mechanisms are mounted on the Kresling tower, on one out of two mountain folds. They are not linked to the panels to avoid any restriction in the motion of the Kresling tower. Each mechanism must act along the axis of the fold. To explain the proposed operating principle, we first consider a perfectly rigid mechanism. The corresponding use is described in Fig. 6. When the Kresling tower is in one of its two stable configurations (Fig. 6.a.), the mechanism can be activated to suppress the relative motion of the fold vertices, needed during the tower motion. In that situation, the Kresling tower becomes fully rigid. To move away from one stable configuration, as shown in Fig. 6 b., the mechanism is deactivated. The tower can then be used normally, with an external action to move the effector. During the tower motion, there is a relative displacement of the fold vertices. One can note that the locking component (in red on Fig. 6) must be at a distance at least equal to this displacement from the base of the mechanism (in blue) to avoid any constraint on the tower.

The stiffening mechanism, and in particular its actuator, cannot be perfectly rigid. The stiffness of the actuator selected to activate the mechanism impacts the modification of the Kresling tower behavior. With compliant actuators, it will be indeed possible to switch between stable configurations while the stiffness mechanisms are activated, but the tower behavior will be modified by the mechanism compliance. In other words, the compliance level of the actuator should allow for different types of changes on the tower force-height relation. At the same time, the interaction forces between the mechanism and the tower will also vary depending on the stiffness of the mechanism.

B. Actuation strategies

Three distinct solutions are considered to assess the importance of the actuation type, namely pneumatic actuation, use of shape memory alloy (SMA) wires, and DC motor actuation. They are chosen to be very different in terms of stiffness, dynamics and technologies, while being of a

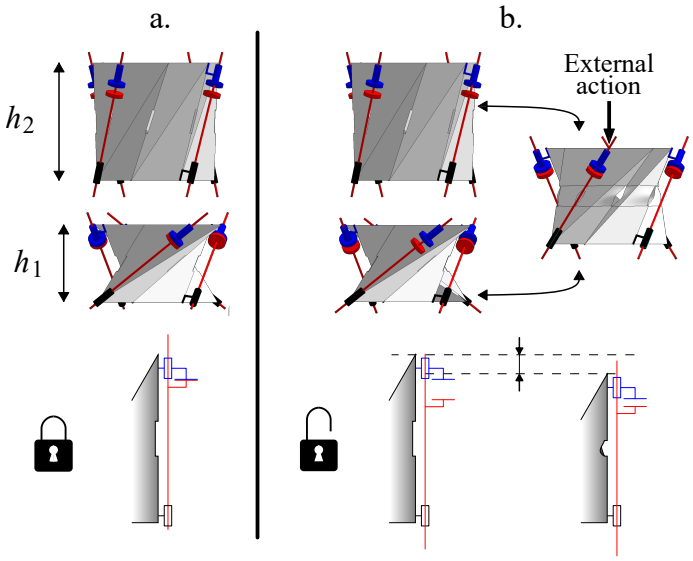

Fig. 6. Principle of the use of stiffening mechanisms.

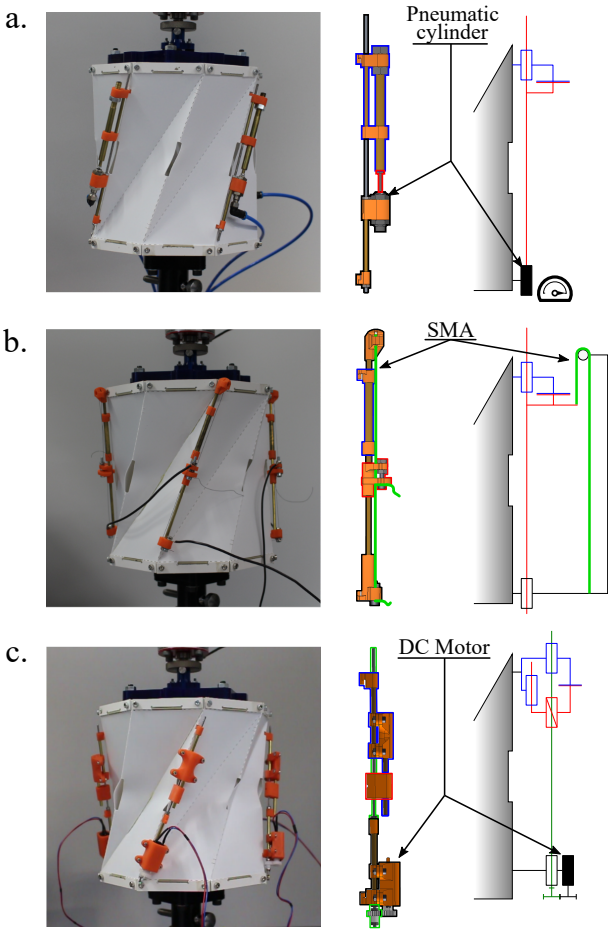

Fig. 7. Design of stiffening mechanisms with a) pneumatic actuation, b) SMA wires, c) DC motors. For each mechanism: modified Kresling tower (left), simplified CAD representation (middle) and kinematic scheme (right). Color codes for the kinematic scheme are reported on the CAD view.

compactness and mass compatible with future integration on a Kresling tower.

Pneumatic actuation offers a significant level of compliance, thanks to air compressibility. For implementation (Fig. 7a.), a standard single-effect small size cylinder is used (CJPB4-10, SMC Corp.). Activation is obtained by applying pressure in the cylinder to get stiffening. Initial testing of the tower shows the relative displacement of fold vertices is about 8 mm. The cylinder stroke is accordingly chosen equal to 10 mm. Activation is quasi-instantaneous, and the motion during deactivation is obtained thanks to the spring of the pneumatic cylinder. With this solution, it is possible to modulate the pressure (up to 7 bars) and hence the force applied along the fold.

The second type of actuation is based on SMA wires, well known for their compactness. For implementation (Fig. 7b.), 375 µm wires are used (Flexinol LT 375 µm, Muscle Wires®). They have a deformation under thermal activation with Joule effect of 3-5% and pulling force of 22 N, according to the manufacturer. For integration, a pulley is added to use the SMA wire contraction to get the stiffening effect. As long as the wire is hot, the tower is stiffened by the SMA wire. Activation time is longer than with pneumatic actuation, measured to be in the order of 10 seconds, if we consider the required cooling time. The motion during deactivation is ensured by introducing manually an initial pretension of the SMA wire.

Finally, a DC motor actuation is considered. For implementation (Fig. 7c.), a screw-nut transmission is used. The motor (RS Pro 834-7647) is a 0.3 W geared DC motor that can generate a torque of 35 N.mm. The screw-nut system is non backdrivable and the overall transmission much stiffer than with the other two actuation strategies. The motor is connected through a pair of gears to avoid collisions with the panels and folds. The reduction ratio related to these gears is 0.83. To set the mechanism in active state, the motor rotates to bring the red part into contact with the blue one. Once in contact, a current measurement of the motors is used to ensure a certain torque and then power is switched off. Then, to set the mechanism in inactive state, the motor is used to back off the red part, using a timer to end the motor rotation. The mechanism needs about 3 minutes to go from its inactive state to its active state.

IV. Experimental Characterization

A. Protocol

The Kresling tower behavior is being evaluated using a tensile test machine (Zwick/Roell, Z005). The relative motion between the base and the effector of the tower is an helical motion. It was observed that the parallelism between them can slightly vary during the tower motion. Thus, a specific set-up is built to connect the Kresling tower with the testing machine (Fig. 8). It is composed of a spherical joint serially connected to a planar joint. Tension-compression cycles can then be applied to the tower prototypes, controlling the tower height. The range of displacement is chosen to make sure we start above the high tower height h_2 and go

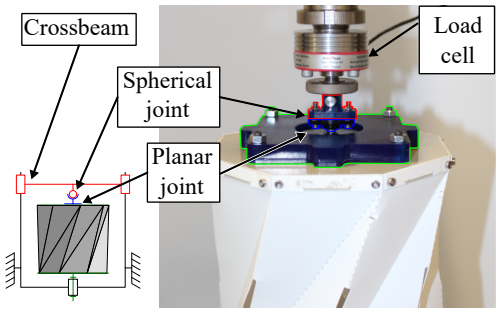

Fig. 8. Interface between the Kresling tower and the tensile test machine.

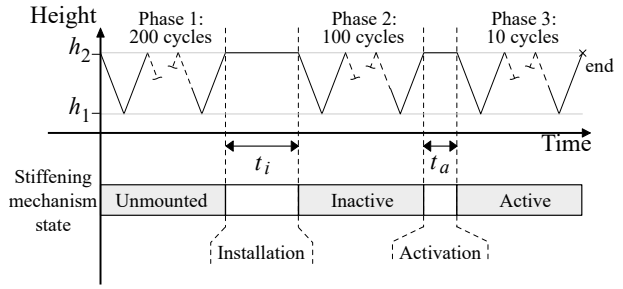

Fig. 9. Simplified representation of the experimental protocol for assessment of stiffening mechanism impact.

below the low height h_1. The speed control of the crossbeam is set at 500 mm/min.

PP viscoelasticity was outlined in [23]. It was handled in the first experimental phase by using identical conditions for all prototypes. Here, the stiffening mechanisms have rather different activation times, so the experimental protocol (Fig. 9) is built to avoid any bias. The protocol is composed of 3 phases. First, a 200-cycle running-in procedure is performed. The stiffening mechanisms are then mounted. A time t_i of 2 hours is allocated to this operation. The second phase aims at stabilizing the behavior of the tower. The tower is submitted to 100 cycles, which allows us to see an established steady-state behavior. The last cycle is exploited to assess the tower. Then the 4 stiffening mechanisms installed on the prototype are activated. The activation time is denoted t_a. After activation, 10 cycles are carried out in order to assess again the tower while the mechanisms are activated.

As outlined in Fig. 4, 6 values of interest are estimated from force-height curves: the heights for stable configurations (h_1 and h_2), the stiffness around these configurations (k_1 and k_2) and also the switching force SF_{21} (resp. SF_{12} to go from h_1 (h_2) to h_2 (h_1). They are obtained by determining points 1 to 4 on Fig. 4.

The activation time may bias the assessment, because of the PP relaxation. For each prototype, the protocol is thus also performed for the tower without the stiffening mechanisms, using the corresponding activation time t_a as a rest time. All results given in Table II are obtained after substracting the variation of switching force, stiffness and stable configuration position which is then measured and due to the PP nonlinearity.

B. Results

The results are gathered in Table II. For height measurements, the differences Δh_1 and Δh_2 between measured and computed values using model in [19] are reported. For pneumatic actuation, it was possible to have repeatedly a transition between the two stable configurations without deactivation of the stiffening mechanisms. This was not the case for SMA and DC motor actuation. Breakage of some connecting elements with the Kresling tower occurred after 3 cycles for SMA actuation, and 1 cycle for DC motor actuation. The results are computed accordingly, by using the Kresling tower after the same number of cycles to compensate for the impact of activation time described above. The force-height relationships for the three actuation strategies are represented in Fig. 10, 11 and 12. For DC motor actuation, a slight discontinuity can be observed around h=125 mm. That corresponds to the breakage of a connecting element after recording point 4 (Fig. 4) so all characteristics of interest are available.

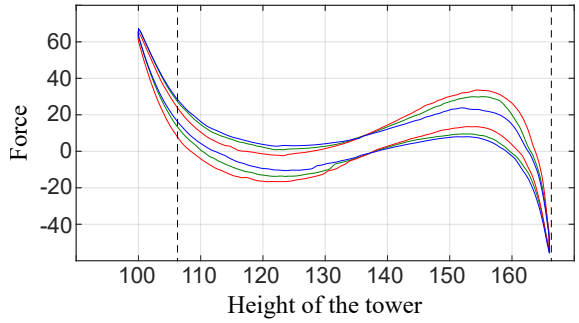

Fig. 10. Experimental results with the pneumatic actuator. Results with the inactive mechanism in blue, in green with activation at a pressure of 4 bars and in red with a pressure of 7 bars. Dashed lines correspond to the theoretical value of stable configurations.

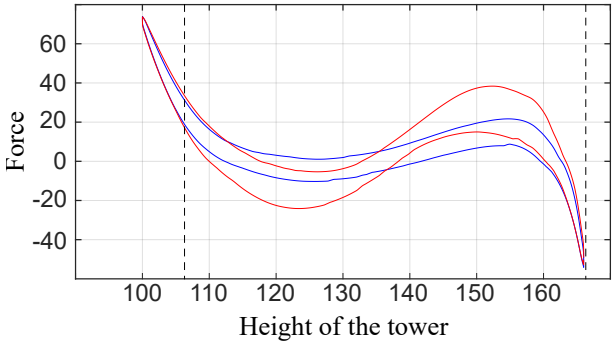

Fig. 11. Experimental results with the SMA-based actuation. Results with the inactive mechanism in blue, in red with activation. Dashed lines correspond to the theoretical value of stable configurations.

C. Discussion

All the mechanisms presented in this paper have a significant impact on the kinetostatic behavior of the Kresling tower. First, for all solutions, the positions of stable configurations h_1 and h_2 are closer, after activation, to the values

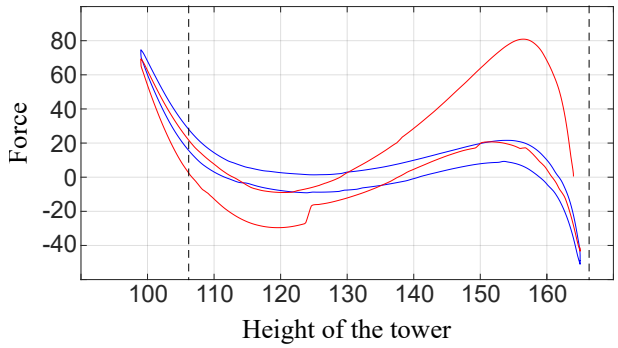

Fig. 12. Experimental results with the DC motor actuation. Results with the inactive mechanism in blue, in red with activation. Dashed lines correspond to the theoretical value of stable configurations.

TABLE II

EXPERIMENTAL RESULTS WITH THE 3 ACTUATION STRATEGIES.

	Δh_2	Δh_1	k_2	k_1	SF_{21}	SF_{12}
	$[mm]$		$[N/mm]$		$[N]$	
Pneumatic actuation						
Inactive	3.7	6.0	4.9	1.4	21.5	-10.6
Active (4bars)	3.3	4.0	5.8	2.4	30.0	-13.8
Active (7bars)	2.5	2.1	9.0	2.6	33.4	-16.9
Impact (4bars)	11%	33%	19%	74%	26%	30%
Impact (7bars)	32%	65%	83%	89%	40%	59%
SMA actuation						
Inactive	3.6	6.0	5.0	1.5	21.6	-10.3
Active	3.2	3.8	6.7	3.1	37.2	-24.1
Impact	17%	37%	34%	107%	72%	134%
DC motor actuation						
Inactive	4.5	5.3	5.3	1.5	21.6	-9.2
Active	4.1	0.6	108.3	4.3	67.2	-29.0
Impact	9%	88%	1953%	190%	211%	217%

computed during design with [19]. Even though the relative errors before stiffening are relatively low, in the order of 5%, this means the presence of stiffening mechanisms helps in improving the prediction accuracy of the Kresling tower model. Embedding active mechanisms along the folds seems helpful, especially for the low configuration. With DC motor actuation the error is in particular almost cancelled.

The switching force is increased with all solutions and in both operating directions of the tower. The increase of the switching force is correlated with the stiffness of the actuator used by the mechanism. This causes also an increase of interaction forces, which explains damage of mechanisms for the 2 stiffest mechanisms when they remain activated during tower motion. The switching force value in both directions is tripled with DC motor actuation. The pneumatic actuation makes it possible to vary the gain in stiffness according to the operating pressure. The SMA-based actuation has a significant impact, while of low size and weight.

Concerning the stiffness around the two stable configurations, the gain can be very important: the DC motor actuated stiffening mechanism multiplies by 20 the stiffness around the high configuration. This mechanism to be used as a locking solution, to prevent configuration switch from occurring. Concerning the stiffening mechanism with SMA actuation, we note a relatively low stiffness increase in the high configuration. In addition, the integration of SMA wires is more delicate because of its behavior when in interaction with a compliant element, such as the origami fold. For that solution, the mechanical backlash present in the prototype may explain the lower impact. As for the switching force, the progressive addition of pressure in the cylinder makes it possible to gradually add stiffness in the stable configurations.

The towers with their rigid ends have a weight approximately equal to 5.6 N. The mechanism integration causes a weight increase between 1.1 and 1.6 N, depending on the actuation strategy. In any case, the value of SF_{21} is increased by 11.9 N and up to 45.6 N when the mechanisms are activated. The contribution to the load capacity seems of interest compared to the relative increase of weight.

We note that the modification on Kresling tower characteristics brought by the stiffening mechanisms are always more important for the low configuration than for the high one. That can be related to fold deformation, which is visually higher in that situation. This behavior may however be linked to the choice of the kinematics of the tower.

V. CONCLUSION

In this paper, we show that it is possible to modify the stiffness and more generally the kinetostatic properties of Kresling tower by embedding active mechanisms along some folds. Axial stiffness modification of folds has a strong impact on stiffness and switching force. With the model of [19], the pattern of the structure can be defined according to the geometrical or kinematic needs. The switching force is then independent from the pattern and the material thanks to the fold opening. The addition of stiffening mechanism makes it possible to modulate the kinetostatic behavior of the structure actively. This set of tools allows to increase the integration capacity of the Kresling tower in more complex robotic systems with various needs.

This work opens several perspectives. First, it will be interesting to model the impact of the stiffening mechanisms, to elaborate a synthesis method of these modified Kresling towers. This will include the assessment of bending stiffness, while axial behavior was the focus here. Second, we will consider further miniaturization of the stiffening mechanisms to design active structural components built as safety components, as described in the introduction. Finally, the use of the proposed stiffening approach will try to be transposed to other non-rigidly foldable origamis.

VI. ACKNOWLEDGEMENT

The authors would like to thank INSA Strasbourg for the access to manufacturing and testing facilities of the Kresling towers presented in this paper.

REFERENCES

[1] R. Phummapooti, N. Jamroonpan, P. Polchankajorn, E. Pengwang, and T. Maneewarn, "Paper-based modular origami gripper," in *2019 IEEE/RSJ International Conference on Intelligent Robots and Systems (IROS)*, (Macau, China), pp. 5614–5619, IEEE, Nov. 2019.

[2] O. Angatkina, B. Chien, A. Pagano, T. Yan, A. Alleyne, S. Tawfick, and A. Wissa, "A metameric crawling robot enabled by origami and smart materials," in *Smart Materials, Adaptive Structures and Intelligent Systems*, vol. 58257, p. V001T06A008, American Society of Mechanical Engineers, 2017.

[3] B. Sargent, J. Butler, K. Seymour, D. Bailey, B. Jensen, S. Magleby, and L. Howell, "An Origami-Based Medical Support System to Mitigate Flexible Shaft Buckling," *Journal of Mechanisms and Robotics*, vol. 12, p. 041005, Aug. 2020.

[4] S. Mintchev, M. Salerno, A. Cherpillod, S. Scaduto, and J. Paik, "A portable three-degrees-of-freedom force feedback origami robot for human–robot interactions," *Nature Machine Intelligence*, vol. 1, pp. 584–593, Dec. 2019.

[5] C. D. Onal, M. T. Tolley, R. J. Wood, and D. Rus, "Origami-Inspired Printed Robots," *IEEE/ASME Transactions on Mechatronics*, vol. 20, pp. 2214–2221, Oct. 2015.

[6] D.-Y. Lee, J.-S. Kim, S.-R. Kim, J.-S. Koh, and K.-J. Cho, "The Deformable Wheel Robot Using Magic-Ball Origami Structure," in *Volume 6B: 37th Mechanisms and Robotics Conference*, (Portland, Oregon, USA), p. V06BT07A040, American Society of Mechanical Engineers, Aug. 2013.

[7] R. J. Lang, *Twists, tilings, and tessellations: mathematical methods for geometric origami*. Boca Raton: CRC Press, Taylor & Francis Group, 2018.

[8] H. Zhang, B. Zhu, and X. Zhang, "Origami Kaleidocycle-Inspired Symmetric Multistable Compliant Mechanisms," *Journal of Mechanisms and Robotics*, vol. 11, p. 011009, Feb. 2019.

[9] A. Pagano, B. Leung, B. Chien, T. Yan, A. Wissa, and S. Tawfick, "Multi-Stable Origami Structure for Crawling Locomotion," in *Smart Materials, Adaptive Structures and Intelligent Systems*, vol. 50497, (Stowe, Vermont, USA), p. V002T06A005, American Society of Mechanical Engineers, Sept. 2016.

[10] N. Kidambi and K. W. Wang, "Dynamics of Kresling Origami Deployment," *Physical Review E*, vol. 101, p. 063003, June 2020. arXiv: 2003.10411.

[11] C. Jianguo, D. Xiaowei, Z. Yuting, F. Jian, and Z. Ya, "Folding Behavior of a Foldable Prismatic Mast With Kresling Origami Pattern," *Journal of Mechanisms and Robotics*, vol. 8, p. 031004, June 2016.

[12] K. Liu and G. Paulino, "Nonlinear mechanics of non-rigid origami: an efficient computational approach," in *Proceedings of the Royal Society A: Mathematical, Physical and Engineering Sciences*, vol. 473:20170348, The Royal Society Publishing, 2017.

[13] S. Li, J. J. Stampfli, H. J. Xu, E. Malkin, E. V. Diaz, D. Rus, and R. J. Wood, "A vacuum-driven origami "magic-ball" soft gripper," in *2019 International Conference on Robotics and Automation (ICRA)*, pp. 7401–7408, 2019.

[14] A. R. Deshpande, Z. T. Ho Tse, and H. Ren, "Origami-inspired bi-directional soft pneumatic actuator with integrated variable stiffness mechanism," in *2017 18th International Conference on Advanced Robotics (ICAR)*, (Hong Kong), pp. 417–421, IEEE, July 2017.

[15] J. Kim, D.-Y. Lee, S.-R. Kim, and K.-J. Cho, "A self-deployable origami structure with locking mechanism induced by buckling effect," in *2015 IEEE International Conference on Robotics and Automation (ICRA)*, (Seattle, WA, USA), pp. 3166–3171, IEEE, May 2015.

[16] F. Zuliani and J. Paik, "Variable Stiffness Folding Joints for Haptic Feedback," in *2021 IEEE/RSJ International Conference on Intelligent Robots and Systems (IROS)*, (Prague, Czech Republic), pp. 8332–8338, IEEE, Sept. 2021.

[17] A. Firouzeh and J. Paik, "An under-actuated origami gripper with adjustable stiffness joints for multiple grasp modes," *Smart Materials and Structures*, vol. 26, no. 5, p. 055035, 2017.

[18] E. Lerner, H. Zhang, and J. Zhao, "Design and Experimentation of a Variable Stiffness Bistable Gripper," in *2020 IEEE/RSJ International Conference on Intelligent Robots and Systems (IROS)*, (Las Vegas, NV, USA), pp. 9925–9931, IEEE, Oct. 2020.

[19] J. Berre, F. Geiskopf, L. Rubbert, and P. Renaud, "Toward the Design of Kresling Tower Origami As a Compliant Building Block," *Journal of Mechanisms and Robotics*, vol. 14, p. 045002, Feb. 2022.

[20] J.-J. Park, B.-S. Kim, J.-B. Song, and H.-S. Kim, "Safe link mechanism based on nonlinear stiffness for collision safety," *Mechanism and Machine Theory*, vol. 43, pp. 1332–1348, Oct. 2008.

[21] H. Yasuda, K. Johnson, V. Arroyos, K. Yamaguchi, J. R. Raney, and J. Yang, "Leaf-Like Origami with Bistability for Self-Adaptive Grasping Motions," *Soft Robotics*, p. soro.2021.0008, Apr. 2022.

[22] J. M. Gattas and Z. You, "Quasi-static impact response of alternative origami-core sandwich panels," in *International Design Engineering Technical Conferences and Computers and Information in Engineering Conference*, vol. 55942, p. V06BT07A032, American Society of Mechanical Engineers, 2013.

[23] A. Drozdov and R. Gupta, "Non-linear viscoelasticity and viscoplasticity of isotactic polypropylene," *International Journal of Engineering Science*, vol. 41, no. 20, pp. 2335–2361, 2003.